

Shape Adaptive All Phase Biorthogonal Transform and Its Application in Image Coding

Baochen Jiang^{1,2}, Aiping Yang¹, Chengyou Wang², and Zhengxin Hou^{1*}

¹ School of Electronic Information Engineering, Tianjin University, Tianjin 300072, P. R. China

² School of Mechanical, Electrical and Information Engineering, Shandong University, Weihai 264209, P. R. China

Email: jbc@sdu.edu.cn; yangaiping@tju.edu.cn; wangchengyou@sdu.edu.cn; zhengxinhou@163.com

Abstract—In this paper shape adaptive all phase biorthogonal transform (SA-APBT) for coding arbitrarily shaped image segments is proposed. The proposed transform can be used in region-based image compression instead of the shape adaptive discrete cosine transform (SA-DCT). Region-based image coding method is made up of three procedures: image segmentation, contour coding and texture coding. An image is divided into region-of-interest (ROI) and background area by image segmentation. Both areas are encoded and decoded independently. Experimental results on test images show that compared with SA-DCT at the same bit rates, the PSNRs and visual effects of reconstructed images based on SA-APBT are comparable to the one based on SA-DCT especially at low bit rates. And the SA-APBT transform coefficients are quantized uniformly, while the SA-DCT transform coefficients are quantized according to different quantization steps in the quantization table. So the quantization based on SA-APBT is simpler and computational complexity is reduced.

Index Terms—image coding, discrete cosine transform (DCT), all phase biorthogonal transform (APBT), shape adaptive, region-of-interest (ROI)

I. INTRODUCTION

Now the orthogonal transformation theory has developed very mature especially the discrete cosine transform (DCT) has been used widely in image and video compression standards. DCT transform has many advantages in terms of energy compaction and coefficients decorrelation [1], but there are also some disadvantages such as the complex quantization table and serious blocking artifacts at low bit rates. To solve these problems, the all phase biorthogonal transform (APBT) which is based on Walsh-Hadamard transform (WHT), DCT and inverse discrete cosine transform (IDCT) was presented and used in image compression instead of DCT [2], [3]. Consequently, the image compression algorithm based on APBT with simpler quantization table improves the performance at low bit rates both in objective effects and subjective effects compared with that based on DCT [3].

However, these standard block-based coding methods have shown many shortcomings such as blocking and ringing effects especially in applications of low bit rates, which promotes the development of region-based image compression [4]. Region-based image coding method which can improve the quality of coded images is made up of three procedures: image segmentation, contour coding and texture coding. Firstly, an image is divided into region-of-interest (ROI) and background area by image segmentation. Both areas are encoded independently. So the decoder can decode and manipulate region-of-interest or background area from bit stream. The shape adaptive DCT (SA-DCT) proposed by Sikora et al. is a transform approach for arbitrarily shaped image segments [5]. Since put forward earlier, the low complexity SA-DCT has been used in many region-based coding systems and included in MPEG 4 video standard verification model [6]. But the reconstructed images based on SA-DCT have obvious block effects at low bit rates. So on the basis of the image compression based on APBT performs better than the one based on DCT at low bit rates [3], shape adaptive all phase biorthogonal transform (SA-APBT) is proposed for arbitrarily shaped image segments instead of SA-DCT in this paper. Experimental results show that compared to SA-DCT at the same bit rates, the PSNRs and reconstructed image effects based on SA-APBT are comparable to SA-DCT especially at low bit rates. In addition, the quantization table based on SA-APBT is simpler and computational complexity is reduced.

The rest of this paper is organized as follows. Section II briefly introduces APBT and JPEG-like image compression algorithm based on the APBT. SA-APBT for coding arbitrarily shaped image segments is explained in Section III. And then in Section IV, region-based image coding using SA-APBT is proposed. Contour coding and texture coding including region-of-interest and background area are described in detail. In order to explain clearly the process of region-based image coding using SA-APBT, an example of 8×8 image block is presented. Experimental results and comparisons between the algorithm based on SA-DCT and the one based on SA-APBT are given in Section V. The rate distortion curves are plotted and some reconstructed images are displayed. Conclusions of the paper and discussion for future work are given in Section VI.

Manuscript received May 6, 2013; revised May 24, 2013.

This work was supported by the National Nature Science Foundation of China under Grant No. 61201371 and No. 61002027.

Corresponding author email: zhengxinhou@163.com.

doi:10.12720/jcm.8.5.330-336

II. ALL PHASE BIORTHOGONAL TRANSFORM (APBT)

On the basis of all phase digital filtering [2], three kinds of all phase biorthogonal transforms based on the WHT, DCT and IDCT were proposed and the matrices of APBT were deduced in [3]. For example, the matrix V of the all phase inverse discrete cosine biorthogonal transform (APIDCBT) is

$$V(m,n) = \begin{cases} \frac{1}{N}, & m=0, n=0,1,\dots,N-1, \\ \frac{N-m+\sqrt{2}-1}{N^2} \cos \frac{m(2n+1)\pi}{2N}, & m=1,2,\dots,N-1, \\ & n=0,1,\dots,N-1. \end{cases} \quad (1)$$

Similar to the DCT matrix, it can be used in image compression transforming the image from spatial domain to frequency domain too.

Fig. 1 shows the main procedures for encoding and decoding processes of JPEG-like image compression algorithm based on the APBT [3]. It illustrates the special case of a single-component image; for color image, all processes operate on each image component independently. Substantially the same as basic steps of the baseline JPEG image compression algorithm, there are only differences in the transform step and quantization step.

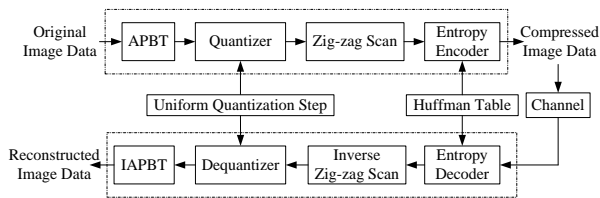


Figure 1. Diagram of the APBT-JPEG image compression algorithm.

In the encoding process, the input image data are grouped into 8×8 blocks, and each block is transformed by the forward APBT into 64 APBT coefficients. One is the DC coefficient and the other 63 are the AC coefficients. Reference [3] indicated that the transform coefficients of APBT have the high-frequency attenuation characteristics, that is to say, the APBT coefficients have different frequency weighted during the transform process. When the transform coefficients are quantized by uniform quantization step, it is equivalent to the low-frequency coefficients are quantized by small step and high-frequency coefficients are quantized by big step. Quantization effects are similar to DCT which adopts complex quantization table. Therefore the uniform quantization step can be applied to the APBT coefficients. After quantization, the APBT coefficients are prepared by zig-zag scan for entropy encoding. The quantized coefficients are then passed to an entropy encoding procedure which compresses the data further. Here, Huffman encoding is used and Huffman table must be provided to the encoder.

In contrast to the encoder, each step of decoding processes performs essentially the inverse of its corresponding main procedure within the encoder. The

entropy decoder decodes the zig-zag sequence of quantized APBT coefficients. After dequantization the APBT coefficients are transformed to an 8×8 block of samples by the inverse APBT (IAPBT). Thus the reconstructed image is obtained.

III. SHAPE ADAPTIVE ALL PHASE BIORTHOGONAL TRANSFORM (SA-APBT)

Just like shape adaptive discrete cosine transform (SA-DCT), the processes of shape adaptive all phase biorthogonal transform (SA-APBT) are comprised of four main procedures: vertical shift, vertical one-dimensional variable-length APBT, horizontal shift and horizontal one-dimensional variable-length APBT. Among three kinds of all phase biorthogonal transforms based on the WHT, DCT and IDCT, the all phase biorthogonal transform based on IDCT (APIDCBT) has the best performance in image compression [3]. So in this paper, the shape adaptive all phase inverse discrete cosine biorthogonal transform (SA-APIDCBT) is mainly introduced and used.

Fig. 2(a) shows an example of a boundary block segmented into foreground (black) and background (white) [5]. Before the pixels in the foreground are vertically shifted, the position of the first pixel of each column in the foreground and the length of each column in the foreground are calculated. Then as is shown in Fig. 2(b), all pixels of each column in the foreground are vertically shifted to the uppermost position according to the calculated shape information. The all shifted pixels in the foreground are grouped into column vector x_j [7].

N_j pixels of each column vector x_j are transformed into N_j vertical transform coefficients by vertical one-dimensional APIDCBT (Fig. 2(c)). The first coefficient in each transform coefficient column vector a_j is the DC coefficient. Based on the position of the first coefficient of each row and the length of each row, the all transform coefficients of each row are horizontally shifted to the left border of the boundary block (Fig. 2(d)). The all shifted transform coefficients are grouped into row vector b_i . Afterwards M_i coefficients of each row vector b_i are transformed into final SA-APIDCBT coefficients by horizontal one-dimensional APIDCBT (Fig. 2(e)). The mathematical expressions of two one-dimensional subtransforms in the vertical and horizontal directions during forward SA-APIDCBT are shown in (2) and (3).

$$a_j = V_{N_j} \cdot x_j, \quad (2)$$

$$c_i = V_{M_i} \cdot b_i, \quad (3)$$

where V_{N_j} and V_{M_i} denote the APIDCBT matrix with length N_j and M_i respectively. Obviously the number of the final SA-APIDCBT coefficients is equal to the number of the pixels in the foreground.

On the basis of the transmitted contour data, the decoder can transform the received SA-APIDCBT coefficients into original foreground data by the inverse SA-APIDCBT. The mathematical expressions of the two one-dimensional subtransforms in the horizontal and vertical directions during inverse SA-APIDCBT are shown in (4) and (5).

$$b_i^* = V_{M_i}' \cdot c_i^* \tag{4}$$

$$x_j^* = V_{N_j}' \cdot a_j^* \tag{5}$$

where the stars indicate the resulting data after the SA-APIDCBT coefficients are quantized and dequantized. The V_{M_i}' and V_{N_j}' denote the inverse APIDCBT matrix V_{M_i} and V_{N_j} respectively.

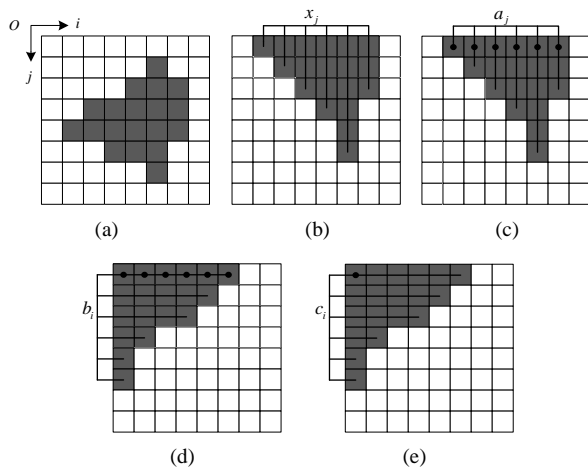


Figure 2. The process of forward SA-APIDCBT on an arbitrarily shaped image segment within an 8x8 block: (a) Original boundary block, (b) Boundary block after the pixels in the foreground are shifted vertically to the upper border, (c) Boundary block after vertical one-dimensional subtransform, (d) Boundary block after the transform coefficients are horizontally shifted to the left border, (e) Final SA-APIDCBT transform coefficients boundary block after horizontal one-dimensional subtransform.

IV. REGION-BASED IMAGE CODING USING SA-APBT

A. Contour Coding

Region-based image coding method is made up of image segmentation, contour coding and texture coding. An image is segmented into region-of-interest and background area manually. After image segmentation, the boundary of the region-of-interest is obtained and is encoded lossless by chain code [5]. To encode the contour data, the connected pixels in region-of-interest are set to black, while collections of pixels in background area are set to white. Two pixels are connected if the square of the distance between them is less than or equal to 2. Then the positions of pixels on the boundary are found clockwise. And the positions of all pixels on the boundary can be expressed by a group directional values of a pixel to next adjacent pixel on the boundary clockwise. The group of directional values are chain codes of the contour of region-of-interest.

There are eight possible directions from one pixel to next adjacent pixel. Fig. 3 shows that the settings of eight direction values in this paper. The processes of contour coding are as follows. Contour coding can start at any pixel on the boundary of region-of-interest. The row and column of the next adjacent pixel on the boundary are found clockwise. Then in the following, the same step proceeds from this new pixel until all pixels on the boundary are found. As a result, the chain codes are obtained according to the difference of row and column of each two adjacent pixels and the settings of chain code direction values.

The process of contour coding for region in Fig. 4 is introduced in detail as follows. The starting point of the boundary is set to the left and upper pixel. Then all pixels on the boundary are found clockwise. Meanwhile the row and column of each pixel on the boundary are recorded. The direction value of two adjacent pixels is obtained according to differences of row and column between the latter pixel and the former one.

- The direction value is 0 if the differences of row and column are 1 and 0.
- The direction value is 1 if the differences of row and column are 1 and 1.
- The direction value is 2 if the differences of row and column are 0 and 1.
- The direction value is 3 if the differences of row and column are -1 and 1.
- The direction value is 4 if the differences of row and column are -1 and 0.
- The direction value is 5 if the differences of row and column are -1 and -1.
- The direction value is 6 if the differences of row and column are 0 and -1.
- The direction value is 7 if the differences of row and column are 1 and -1.

The resulting all direction values are chain codes of contour of region in Fig. 4. So the chain codes are “22110776655433”. Therefore the final binary representation of chain codes are “01001000100100011111110110101101100011011” with each chain code value is represented by three bits.

Finally the row and column of the starting point and chain codes are transmitted to the decoder as contour coding data. The encoded contour data are transmitted prior to the texture coding data of region-of-interest and background area. Therefore the decoder can draw the shape and position of the region-of-interest from the received contour data.

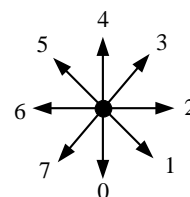


Figure 3. The settings of chain code directions.

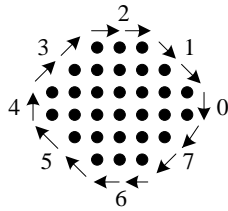


Figure 4. Chain codes of an arbitrarily shaped region.

B. Texture Coding

Texture coding includes region-of-interest texture coding and background area texture coding. These two areas are encoded independently.

Fig. 5 shows the main procedures for the encoding and decoding processes of region-based image coding using SA-APBT. The background area image data are set to zero, when the region-of-interest image data are encoded [8]. Before the region-of-interest image data are encoded, the minimum rectangle whose length and width are multiples of eight including the region-of-interest is found. And the row and column of the left and upper pixel in the minimum rectangle are multiples of eight plus one. Then the pixels in the minimum rectangle are grouped into 8x8 blocks.

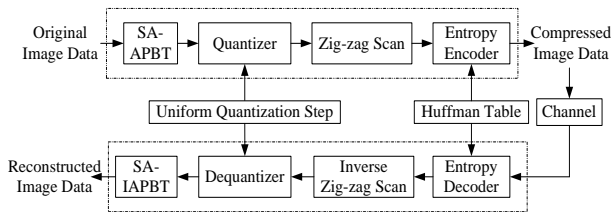


Figure 5. Diagram of the region-based image coding using SA-APBT.

Based on the calculated number of the pixels in the region-of-interest of each block, all 8x8 blocks are divided into three groups:

- a) Each block in the first group with the number equal to zero is not transformed.
- b) Each block in the second group with the number equal to 64 is transformed by APBT into 64 transform coefficients.
- c) Each block in the third group with the number is larger than zero and smaller than 64 is transformed by SA-APBT according to shape information [9].

The resulting each transform coefficient block is quantized by uniform quantization step according to the high-frequency attenuation characteristics of the APBT. After quantization, the SA-APBT coefficients are prepared for entropy encoding. The difference between previous quantized DC coefficient and current quantized DC coefficient is encoded. The 63 quantized AC coefficients are converted into one-dimensional zig-zag sequence and then are entropy encoded. Here, Huffman encoding is used and Huffman table must be provided to the encoder.

In the decoding process, the entropy decoder decodes the zig-zag sequence of quantized SA-APBT coefficients.

Afterwards the quantized SA-APBT coefficients are dequantized into SA-APBT coefficients by uniform quantization step. To perform inverse SA-APBT (SA-IAPBT), the transmitted contour data are calculated. Then the contour of the region-of-interest is recovered. Therefore the minimum rectangle whose length and width are multiples of eight including the region-of-interest is regained according to the recovered contour. The number of pixels of the region-of-interest for each 8x8 block in the minimum rectangle is obtained. Similarly, all blocks are divided into three groups according to the number of pixels of the region-of-interest for each block:

- a) All SA-APBT coefficients in the block of the first group are not inverse transformed.
- b) All SA-APBT coefficients in the block of the second group are transformed by IAPBT.
- c) All SA-APBT coefficients in the block of the third group are transformed by SA-IAPBT.

Now the reconstructed region-of-interest image data are obtained.

The encoding and decoding processes of background area are the same as region-of-interest. The reconstructed full image can be got by merging the reconstructed region-of-interest and background area image data.

C. Example of Region-based Image Coding Using SA-APBT

Taking an image block of 8x8 in gray image Announcer for an example, the process of region-based image coding using SA-APBT is briefly introduced as follows. Fig. 6(a) shows that the original image data of an image block of 8x8. This block is located in the boundary of region-of-interest and background area. When the region-of-interest image data are coded, the image data of background area are set to zero. The image data with value are equal to zero in Fig. 6(a) are background area. The original image block data are transformed by SA-APBT into transform coefficients as shown in Fig. 6(b). Then the resulting SA-APBT coefficients are quantized by uniform quantization step. Fig. 6(c) shows that the quantized SA-APBT coefficients. After entropy encoding and entropy decoding, the quantized SA-APBT coefficients are dequantized by uniform quantization step as shown in Fig. 6(d). Finally Fig. 6(e) shows that the reconstructed image block data obtained by SA-IAPBT.

0	0	0	0	0	0	0	0
0	0	0	0	0	0	0	0
0	0	0	0	101	136	165	176
145	157	154	178	204	198	195	211
206	216	209	205	210	212	210	202
216	214	206	206	208	200	190	181
199	202	205	196	184	181	178	167
188	196	186	182	183	174	167	169

(a)

187.9	2.8	0.2	-1.0	-0.3	0.1	-0.2	-0.2
-2.6	-2.1	1.1	-1.1	0.1	0.4	-0.1	-0.2
-8.4	-0.3	0.7	-1.0	0.0	0.3	-0.1	-0.2
-3.5	0.3	0.1	-0.4	-0.1	0.4	-0.0	-0.1
-1.0	0.1	0.2	-0.0	-0.0	0.1	-0.0	-0.0
-0.5	-0.2	-0.2	0.0	0	0	0	0
0	0	0	0	0	0	0	0
0	0	0	0	0	0	0	0

(b)

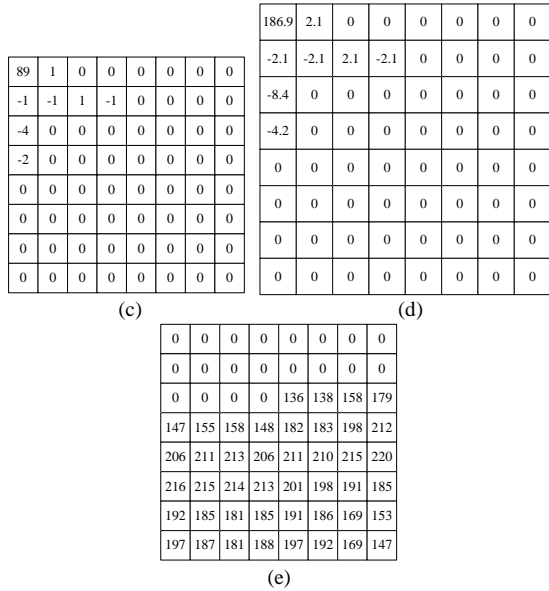


Figure 6. Process of region-based image coding using SA-APBT: (a) Original image data, (b) SA-APBT coefficients, (c) Quantized SA-APBT coefficients, (d) Dequantized SA-APBT coefficients, (e) Reconstructed image data.

V. EXPERIMENTAL RESULTS AND COMPARISONS WITH ALGORITHM BASED ON SA-DCT

In this paper all simulation results are obtained with MATLAB 7.8. To test proposed scheme and compare with region-based image coding using SA-DCT, the typical gray images Announcer and Barbara with size 512x512, 8 bits/pixel are used in experiments. The image coding algorithm based on SA-DCT uses SA-DCT with Δ DC correction scheme [7]. While the image coding algorithm based on SA-APBT uses SA-APBT with Δ DC correction scheme. The distortion is measured by the Peak Signal to Noise Ratio (PSNR)

$$PSNR = 10 \log_{10} \left(\frac{255^2}{MSE} \right) (dB) \tag{6}$$

where MSE denotes the mean squared error between the original and reconstructed images.

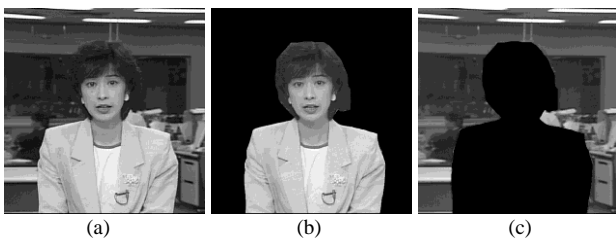


Figure 7. Announcer images: (a) Original image, (b) Region-of-interest, (c) Background area.

Fig. 7 shows that the original Announcer image segmented into region-of-interest (Fig. 7(b)) and background area (Fig. 7(c)). Fig. 8 shows the original Barbara image segmented into region-of-interest (Fig. 8(b)) and background area (Fig. 8(c)). The region-based image coding algorithm using SA-DCT and SA-

APIDCBT both encode region-of-interest and background area independently. Therefore, the decoder can individually decode and manipulate the region-of-interest or background area [5].

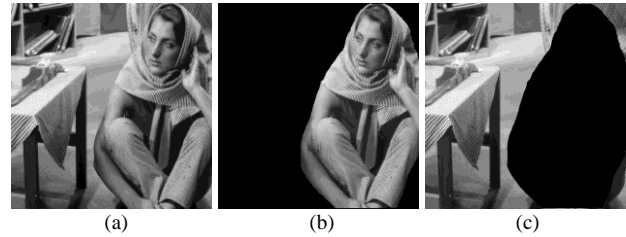


Figure 8. Barbara images: (a) Original image, (b) Region-of-interest, (c) Background area.

Tab. I and Tab. II show that the experimental results of region-based image coding using SA-DCT and SA-APIDCBT in terms of PSNR of reconstructed full image at different bit rates applied to image Announcer and Barbara respectively. All experimental results are obtained under the condition that the quantization matrix of region-of-interest is the same as the background area for both SA-DCT and SA-APIDCBT. The bit rate in Table. I and Table. II is the total bit rate of the full image including contour coding and texture coding.

TABLE I: PSNR COMPARISON OF SA-DCT AND SA-APIDCBT APPLIED TO IMAGE ANNOUNCER

Bit rate (bpp)	SA-DCT		SA-APIDCBT	
	Matrix Q Multiply	PSNR (dB)	Step Q	PSNR (dB)
0.20	6.800	26.91	6.900	31.07
0.30	2.700	33.47	2.560	34.74
0.40	1.580	35.86	1.480	36.68
0.50	1.070	37.52	0.993	37.98
0.60	0.795	38.58	0.725	38.92
0.70	0.628	39.33	0.570	39.64
0.80	0.513	40.05	0.464	40.26

TABLE II: PSNR COMPARISON OF SA-DCT AND SA-APIDCBT APPLIED TO IMAGE BARBARA

Bit rate (bpp)	SA-DCT		SA-APIDCBT	
	Matrix Q Multiply	PSNR (dB)	Step Q	PSNR (dB)
0.30	5.900	24.13	5.600	25.10
0.40	3.950	25.89	3.750	26.64
0.50	2.860	27.38	2.700	28.02
0.60	2.160	28.75	2.030	29.32
0.70	1.680	29.96	1.580	30.50
0.80	1.340	31.04	1.260	31.55
0.90	1.090	32.04	1.030	32.47

From the experimental results in Tab. I and Tab. II, we conclude that compared with the region-based image coding algorithm using SA-DCT in terms of PSNR of reconstructed full image, the performances using SA-APIDCBT are all comparable to that using SA-DCT especially at low bit rates. Based on the data in Tab. I and Tab. II, we plot the rate distortion curves of Announcer and Barbara images using the two transforms, as shown in Fig. 9 (a) and (b).

In order to compare the compression performance subjectively, Fig. 10 shows the reconstructed Announcer images based on SA-DCT and SA-APIDCBT when the total encoding bit-rate is 0.30bpp and the two areas including region-of-interest and background area are encoded with the same quantization matrix for both SA-DCT and SA-APIDCBT. Fig. 11 shows the reconstructed Barbara images based on SA-DCT and SA-APIDCBT when the total encoding bit-rate is 0.40bpp and the two areas including region-of-interest and background area are encoded with the same quantization matrix for both SA-DCT and SA-APIDCBT. It can be seen that the block artifacts of reconstructed Announcer and Barbara images based on SA-DCT are apparent. Compared with region-based image coding algorithm using SA-DCT, the block artifacts of reconstructed Announcer and Barbara images based on SA-APIDCBT are reduced greatly and the subjective effects are better.

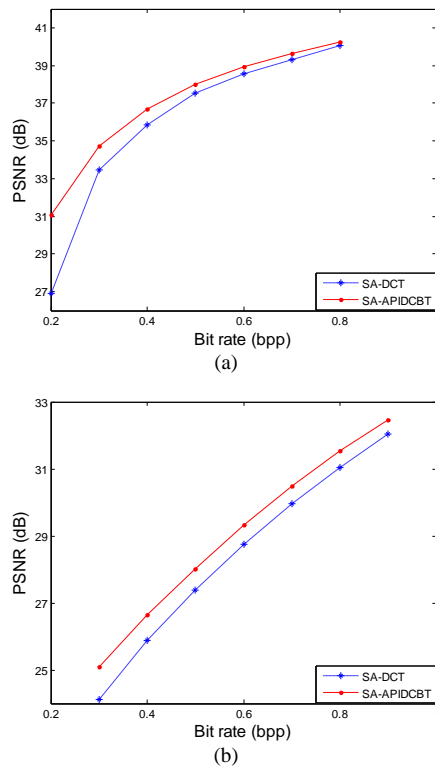


Figure 9. Rate distortion curves: (a) Announcer, (b) Barbara.

To save the total encoding bit rate and take advantage of the vision characteristics of human eyes, the region-of-interest can be encoded with increased quality and the background area can be encoded with reduced quality.

Fig. 12(a) shows the reconstructed Announcer image based on SA-DCT under the condition that total encoding bit-rate is 0.30bpp when the quantization matrix of region-of-interest is $Q*2.30$ and the quantization matrix of background area is $Q*3.18$. Fig. 12(b) shows the reconstructed Announcer image based on SA-APIDCBT under the condition that total encoding bit-rate is 0.30bpp when the quantization step of region-of-interest is 2.10 and the quantization step of background area is 3.13. Apparently the region-of-interest is coded with increased quality and background area is coded with reduced quality.

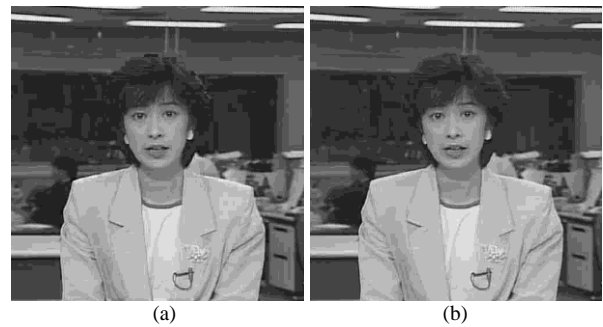


Figure 10. Reconstructed Announcer images (0.30bpp): (a) SA-DCT, (b) SA-APIDCBT.

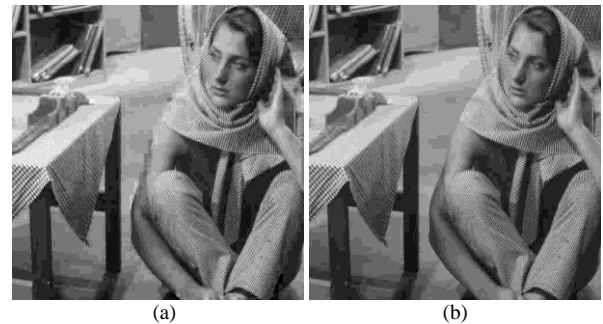


Figure 11. Reconstructed Barbara images (0.40bpp): (a) SA-DCT, (b) SA-APIDCBT.



Figure 12. Reconstructed Announcer images in which region-of-interest is encoded with increased quality and background area is encoded with reduced quality: (a) SA-DCT, (b) SA-APIDCBT.

In conclusion, compared with region-based image coding algorithm using SA-DCT, the algorithm based on SA-APIDCBT performs better both in terms of PSNR and subjective effects. And each image block using SA-APIDCBT can save 63 multiplication operations between quantization factor and quantization table because of the

use of uniform quantization step, when adjusting encoding bit rates.

VI. CONCLUSIONS

In this paper, the shape adaptive all phase biorthogonal transform (SA-APBT) for coding arbitrarily shaped image segments is proposed. The region-based image coding is made up of image segmentation, contour coding and texture coding which includes region-of-interest and background area texture coding. To save the total encoding bit rate and take advantage of the vision characteristics of human eyes, the region-of-interest is encoded with increased quality and the background area is encoded with reduced quality. The PSNR of reconstructed images and subjective effects based on the proposed algorithm are comparable to the one based on SA-DCT especially at low bit rates.

The advantage of the proposed algorithm is using uniform quantization step, and saving multiplication operations between quantization factor and quantization table when adjusting encoding bit rates. So it is easier for image compression and to implement by hardware. We can continue to explore other applications of SA-APBT in MPEG-4 video compression. These issues are left for future research.

ACKNOWLEDGMENT

This work was supported by the National Nature Science Foundation of China (Grant No. 61201371, No. 61002027). The authors would like to thank Xiaoyan Wang and Chunxiao Zhang for their help and valuable suggestions. The authors also thank the anonymous reviewers and the editor for their valuable comments to improve the presentation of the paper.

REFERENCES

- [1] E. C. Acocella and A. Alcaim, "Alignment by phase of vertical coefficients in SA-DCT," *IEEE Signal Processing Letters*, vol. 8, no. 2, pp. 42-44, Feb 2001.
- [2] Z. X. Hou and X. Yang, "The all phase DFT filter," in *Proc. 10th IEEE Digital Signal Processing Workshop and the 2nd IEEE Signal Processing Education Workshop*, Pine Mountain, Georgia, USA, Oct 2002, pp. 221-226.
- [3] Z. X. Hou, C. Y. Wang, and A. P. Yang, "All phase biorthogonal transform and its application in JPEG-like image compression," *Signal Processing: Image Communication*, vol. 24, no. 10, pp. 791-802, Nov 2009.
- [4] S. Makrogiannis, P. Schelkens, S. Fotopoulos, and J. Cornelis, "Region-oriented compression of color images using fuzzy inference and shape adaptive DCT," in *Proc. IEEE Int. Conf. on*

Image Processing, Thessaloniki, Greece, Oct 2001, vol. 3, pp. 478-481.

- [5] T. Sikora, "Low complexity shape-adaptive DCT for coding of arbitrarily shaped image segments," *Signal Processing: Image Communication*, vol. 7, no. 4-6, pp. 381-395, Nov 1995.
- [6] ISO/IEC JTC1/SC29, Information technology – Generic coding of audio-visual objects: Part 2 – Visual, *ISO/IEC 14496-2*, Jan. 2000.
- [7] P. Kauff and K. Schuur, "Shape-adaptive DCT with block-based DC separation and Δ DC correction," *IEEE Trans. on Circuits and Systems for Video Technology*, vol. 8, no. 3, pp. 237-242, Jun 1998.
- [8] K. Belloulata, R. Stasinski, and J. Konrad, "Region-based image compression using fractals and shape-adaptive DCT," in *Proc. Int. Conf. on Image Processing*, Kobe, Japan, Oct. 1999, vol. 2, pp. 815-819.
- [9] T. Sikora and B. Makai, "Shape-adaptive DCT for generic coding of video," *IEEE Trans. on Circuits and Systems for Video Technology*, vol. 5, no. 1, pp. 59-62, Feb 1995.



Baochen Jiang received his B.S. degree in radio electronics from Shandong University, China, in 1983 and his M.E. degree in communication and electronic systems from Tsinghua University, China, in 1990. Now he is a professor in Shandong University, Weihai, China. His current research interests include signal and information processing, image and video compression, and smart grid technology.



Aiping Yang received her B.Ed. degree in mathematics education from Shandong Normal University, China, in 2000 and her M.S. degree in operations research and control theory from Tianjin University, China, in 2003 and her Ph.D. degree in signal and information processing from Tianjin University, China, in 2008. Now she is an associate professor in Tianjin University, China. Her current research interests include digital

image and video processing, compressive sensing theory, and wavelet analysis.



Chengyou Wang received his B.E. degree in electronic information engineering from Yantai University, China, in 2004 and his M.E. and Ph.D. degree in signal and information processing from Tianjin University, China, in 2007 and 2010 respectively. Now he is a lecturer in Shandong University, Weihai, China. His current research interests include digital image and video processing, wavelet analysis and its applications, and smart grid technology.



Zhengxin Hou received the B.E. degree in electrical engineering from Peking University, China, in 1969 and the M.E. degree from Tianjin University, China, in 1982. Now he is a professor and supervisor of the Ph.D. students in Tianjin University, China. His current research interests include digital filtering theory, digital image and video processing, and wavelet analysis.